Polarization-sensitive IR-pump–x-ray-probe spectroscopy

Ji-Cai Liu [1,*] Viktoriia Savchenko [2,3] Victor Kimberg [2,3,†] Michael Odelius [4] and Faris Gel'mukhanov[2,3,5,6]

[1]*Department of Mathematics and Physics, North China Electric Power University, 102206 Beijing, China*
[2]*Department of Theoretical Chemistry and Biology, KTH Royal Institute of Technology, 10691 Stockholm, Sweden*
[3]*International Research Center of Spectroscopy and Quantum Chemistry (IRC SQC),*
Siberian Federal University, 660041 Krasnoyarsk, Russia
[4]*Department of Physics, AlbaNova University Center, Stockholm University, SE-106 91 Stockholm, Sweden*
[5]*Kirensky Institute of Physics, Federal Research Center KSC SB RAS, 660036 Krasnoyarsk, Russia*
[6]*Institute for Methods and Instrumentation in Synchrotron Radiation Research FG-ISRR, Helmholtz-Zentrum Berlin*
für Materialien und Energie, Albert-Einstein-Strasse 15, 12489 Berlin, Germany

X-ray absorption and core-ionization spectra of molecules pumped by two coherent infrared pulses with different polarizations are studied theoretically. We have found a sensitivity of the vibrational profile of x-ray probe spectra to polarizations of the IR and x-ray pulses. This polarization dependence is qualitatively different for x-ray absorption and x-ray photoelectron spectra. Measurements of this polarization dependence allow to select the difference in Franck-Condon distributions from the lowest and pumped vibrational levels of the electronic ground state. The proposed technique is exemplified numerically using x-ray absorption spectra of the pumped CO molecule. We also show that this kind of pump-probe spectroscopy can enable studies of the dynamics of molecular rotation.

I. INTRODUCTION

Interactions of intense electromagnetic pulses with matter are attracting increasing interest due to its intrinsic potential to investigate the dynamics of quantum systems in real timescales and because of the possibility to manipulate quantum states. Time-resolved laser pump-probe spectroscopies open perspectives in the studies of dynamical processes in structural chemistry, biology, and the physics of phase transitions [1–3]. The use of polarization sensitive techniques is common in many time-resolved optical pump-probe experiments [4]. In this context, resonant inelastic x-ray scattering (RIXS) can be considered as a special kind of pump-probe spectroscopy. It was recognized that polarization sensitivity of RIXS is a useful tool to study anisotropy of electronic states [5–9]. Time-dependent pump-probe spectroscopy [10–13] turns out to be the adequate setup to study ultrafast quantum dynamics of electrons and nuclei, for example, the motion of the nuclear wave packet in the potential-energy surfaces. IR-pump-x-ray-probe spectroscopy allows to study directly the nuclear dynamics induced by the pump IR field in real

time [14–19]. Here the use of ultrashort coherent x-ray pulses produced at high harmonic generation sources provides a possibility to characterize electronic, vibrational, and rotation dynamics in a single experiment [20,21]. On the other hand, the role of polarization can also be important in IR + x-ray pump-probe spectroscopy. In the present paper, we explore the polarization sensitivity of x-ray absorption and x-ray photoionization of molecules pumped by two coherent, time-delayed, and linearly polarized long IR pulses. The proposed technique is advantageous as it does not require use of ultrashort x-ray pulses, whereas the measurements can be performed even with rather long x-ray pulses from synchrotron radiation facilities.

One should note that the ordinary x-ray absorption spectra (XAS) of randomly oriented molecules do not depend on the polarization of the x rays. The main reason for the polarization sensitivity of IR + x-ray pump-probe absorption spectra is the different orientation of the transition dipoles moments of the IR transition and the electronic transition of core excitation. As we will show, the situation is rather different in the case of x-ray photoelectron spectroscopy (XPS) where the polarization sensitivity of x-ray pump-probe XPS spectra stems from different orientations of the polarization vectors of two coherent IR-pump fields.

The paper is organized as follows. We present the general theoretical framework in Sec. II. We discuss the special role of polarization in Sec. III where the polarization dependence for the case of CO molecule is exemplified, and an average over molecular orientation is taken into account. A possibility of separation of contributions from the ground and pumped vibrational levels to the probe spectra (XAS and XPS) is

*jicailiu@ncepu.edu.cn
†kimberg@kth.se
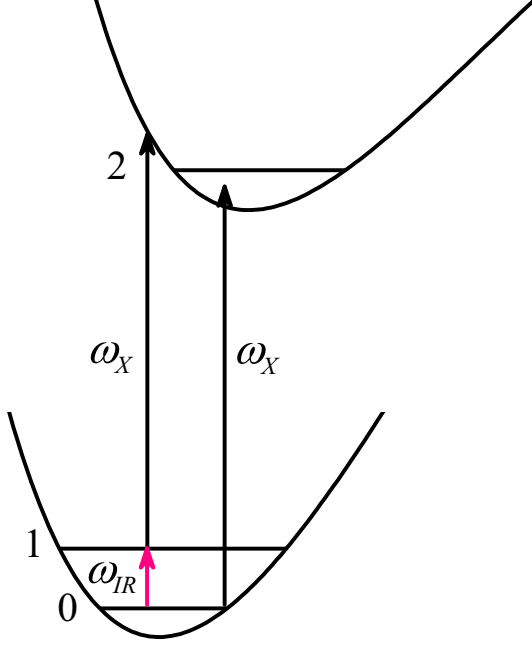
FIG. 1. Qualitative picture of the one- and two-photon channels of core excitation. Labels 0 and 1 denote the two lowest vibrational levels of the ground electronic state mixed by the IR pulse ω_{IR}, whereas label 2 refers to a vibrational resonance in the core-excited (core-ionized) state populated by x-ray pulse ω_X.

discussed in Sec. III D along with a possible experimental scheme. In Sec. III E we discuss the sensitivity of the proposed technique to molecular rotation. Our results are summarized in Sec. IV.

II. THEORY

We consider the interaction of the molecule with the nonoverlapping IR-pump and time-delayed x-ray probe pulses (Fig. 1),

$$\tfrac{1}{2}\mathbf{E}_{\text{IR}}e^{-i\omega_{\text{IR}}t} + \text{c.c.}, \qquad \tfrac{1}{2}\mathbf{E}_X e^{-i\omega_X t} + \text{c.c.} \tag{1}$$

The frequency ω_{IR} of the IR field with duration τ is tuned near the resonance with the frequency ω_{10} of the first vibrational transition $\nu = 0 \rightarrow 1$ of the ground electronic state whereas the frequency ω_X of the x-ray field is tuned near the resonant frequencies ω_{20} and ω_{21} of the transitions from the vibrational states 0 and 1 to the electronically core-excited vibrational state 2. To make the physical picture clear we consider rectangular IR and x-ray pulses, time delayed with respect to each other. Our approach is limited to weak probe and pump pulses. This permits us to employ a perturbative treatment of the two-color x-ray absorption and ionization processes. The wave function of the molecule in the interaction picture $\psi = a_2\psi_2 + a_1\psi_1 + a_0\psi_0$ is the coherent mixture of vibrational states 0, 1, and of the core-excited state 2 where the amplitudes a_n satisfy the following equations in the rotating-wave approximation (in atomic units),

$$\dot{a}_2 + \Gamma a_2 = iG_{21}e^{i(\omega_{21}-\omega_X)t}a_1 + iG_{20}e^{i(\omega_{20}-\omega_X)t}a_0,$$
$$\dot{a}_1 + \gamma a_1 = iG_{10}e^{i(\omega_{10}-\omega_{\text{IR}})t}a_0,$$
$$|a_0|^2 + |a_1|^2 \approx 1,$$

where we, by omitting $G_{12}a_2$ in the equation for a_1, neglect the change in population of level 1 by the weak probe x-ray pulse. Here $G_{2n} = (\mathbf{E}_X \cdot \mathbf{d}_{2n})/2$ and $G_{10} = (\mathbf{E}_{\text{IR}} \cdot \mathbf{d}_{10})/2$ are the Rabi frequencies of x-ray and IR transitions, respectively. One should note that electronic transition dipole moments $\mathbf{d}_{20}$ and $\mathbf{d}_{21}$ are the same (the difference in the vibrational structure is considered in the next section) and the transition dipole moment of IR transition $\mathbf{d}_{10}$ is oriented along molecular axis $\mathbf{R}$ in heteronuclear diatomic molecules. We consider below two XAS channels $1s \rightarrow \sigma^*$ and $1s \rightarrow \pi^*$ with the transition dipole moment $\mathbf{d}_{20} \parallel \mathbf{R}$ and $\mathbf{d}_{20} \perp \mathbf{R}$, respectively.

The IR pulse, switched at $t = 0$, creates population ρ_{11} in vibrational level 1 of the electronic ground state, which at the end of the IR pulse $t = \tau$ reads

$$\rho_{11}(\tau) = |a_1(\tau)|^2,$$
$$a_1(\tau) = G_{10}\frac{e^{i(\omega_{10}-\omega_{\text{IR}})\tau} - e^{-\gamma\tau}}{\omega_{10} - \omega_{\text{IR}} - i\gamma}. \tag{2}$$

When the IR pulse is turned off $t \geqslant \tau$ the system experiences free decay,

$$a_1(t) = a_1(\tau)e^{-\gamma(t-\tau)},$$
$$a_0(t) \approx 1 - \frac{\rho_{11}(\tau)}{2}e^{-2\gamma(t-\tau)}.$$

The second term on the right-hand side of the expression for $a_0(t)$ describes depopulation of the lowest level by the IR pump. Hereafter, the core-excited state is populated by the probe x-ray pulse delayed with respect to the IR pulse by Δt,

$$a_2(t) = \left\{ G_{21}a_1(\tau)\frac{e^{-i\omega_{10}t}e^{-\gamma(t-\tau)}}{\omega_{21} - \omega_X - i\Gamma} \right.$$
$$\left. + \frac{G_{20}}{\omega_{20} - \omega_X - i\Gamma}\left[1 - \frac{\rho_{11}(\tau)}{2}e^{-2\gamma(t-\tau)}\right]\right\}$$
$$\times e^{i(\omega_{20}-\omega_X)t}\Theta(t - t_X),$$

where $t_X \equiv \tau + \Delta t$, $\Theta(t - t_X)$ is the step function equal to zero when $t < t_X$. We assume here that the duration τ_X of the x-ray pulse is longer than the lifetime of the core-excited state $1/\Gamma$ and $\Gamma \gg \gamma$. Taking into account that the lifetime of vibrational state $1/\gamma$ of gas phase molecules is in the range of 10^{-3} s [22] and is usually much longer than the delay time Δt and duration of the x-ray pulse one can replace $e^{-\gamma(t-\tau)}$ by 1. This allows us to write the amplitude of the x-ray absorption and ionization $F \propto a_2$ as follows:

$$F = \left\{ G_{21}a_1(\tau)\frac{e^{-i\omega_{10}t}}{\omega_{21} - \omega_X - i\Gamma} \right.$$
$$\left. + \frac{G_{20}}{\omega_{20} - \omega_X - i\Gamma}\left[1 - \frac{\rho_{11}(\tau)}{2}\right]\right\}\Theta(t - t_X).$$

Thus, the cross section of x-ray absorption and ionization of a molecule driven by the IR field is divided into a sum of partial cross sections of one- and two-photon transitions (σ_0 and σ_1,

respectively) and the interference term σ_{coh},

$$\sigma = |F|^2 = \sigma_0 + \sigma_1 + \sigma_{\text{coh}},$$

$$\sigma_0 = \frac{|G_{20}|^2}{(\omega_X - \omega_{20})^2 + \Gamma^2},$$

$$\sigma_1 = \left(\frac{|G_{21}|^2}{(\omega_X - \omega_{21})^2 + \Gamma^2} - \frac{|G_{20}|^2}{(\omega_X - \omega_{20})^2 + \Gamma^2} \right) \rho_{11}(\tau).$$

$$(3)$$

The interference between one- $(0 \to 2)$ and two-photon $(0 \to 1 \to 2)$ channels,

$$\sigma_{\text{coh}} = 2 \operatorname{Re} \frac{G_{21} G_{20}^* a_1(\tau) e^{-i\omega_{10}t}[1 - \rho_{11}(\tau)/2]}{(\omega_{21} - \omega_X - i\Gamma)(\omega_{20} - \omega_X + i\Gamma)} \quad (4)$$

can be significant only when the duration of x-ray pulse τ_X is comparable to or shorter than period of vibration $\tau_X \omega_{10} \lesssim 1$ and it is strictly equal to zero for randomly oriented molecules [14,15] (see Appendix A). Hence, we neglect σ_{coh} in the analysis below.

III. ROLE OF POLARIZATION

Let us now specify the amplitudes of the IR and x-ray fields (1),

$$\mathbf{E}_{\text{IR}} = E_1 \mathbf{e}_{\text{IR}}^{(1)} + E_2 \mathbf{e}_{\text{IR}}^{(2)} e^{i\varphi}, \quad \mathbf{E}_X = E_X \mathbf{e}_X, \quad (5)$$

assuming that all fields are linearly polarized with polarization vectors $\mathbf{e}_{\text{IR}}^{(1)}$, $\mathbf{e}_{\text{IR}}^{(2)}$, and $\mathbf{e}_X$. The IR field consists of two phase-shifted IR pulses with the same frequency but different polarization vectors $\mathbf{e}_{\text{IR}}^{(1)}$ and $\mathbf{e}_{\text{IR}}^{(2)}$. The reason for the phase shift can be the time-delay (Δt_{IR}) between IR pulses $\varphi = \omega_{\text{IR}} \Delta t_{\text{IR}}$. We assume that both IR pulses have the same envelope. This is valid when $\tau \gg \Delta t_{\text{IR}}$. To get the phase shift $\varphi = \omega_{\text{IR}} \Delta t_{\text{IR}} \approx \pi$ for $\omega_{\text{IR}} \approx 0.2$ eV we need $\Delta t_{\text{IR}} \approx 10$ fs. Thus, our assumption is valid for rather long IR pulses $\tau > 100$ fs.

Since the IR field $\mathbf{E}_{\text{IR}}$ (5) has two components, the square of the Rabi frequency of IR transition G_{10} consists of three contributions,

$$|G_{10}|^2 = \left(G_{10}^{(1)}\right)^2 \left(\mathbf{e}_{\text{IR}}^{(1)} \cdot \hat{\mathbf{d}}_{10}\right)^2 + \left(G_{10}^{(2)}\right)^2 \left(\mathbf{e}_{\text{IR}}^{(2)} \cdot \hat{\mathbf{d}}_{10}\right)^2$$
$$+ 2 G_{10}^{(1)} G_{10}^{(2)} \left(\mathbf{e}_{\text{IR}}^{(1)} \cdot \hat{\mathbf{d}}_{10}\right) \left(\mathbf{e}_{\text{IR}}^{(2)} \cdot \hat{\mathbf{d}}_{10}\right) \cos \varphi,$$

where $G_{10}^{(n)} = E_n d_{10}/2$ and $\hat{\mathbf{d}} = \mathbf{d}/d$ denotes the unit vector along $\mathbf{d}$. Consequently, the population of the excited vibrational level of the ground electronic state (2) reads

$$\rho_{11}(\tau) = \rho_{11}^{(0)}(\tau) + \rho_{11}^{(1)}(\tau) \cos \varphi,$$

$$\rho_{11}^{(0)}(\tau) = \left[\left(G_{10}^{(1)}\right)^2 \left(\mathbf{e}_{\text{IR}}^{(1)} \cdot \hat{\mathbf{d}}_{10}\right)^2 + \left(G_{10}^{(2)}\right)^2 \left(\mathbf{e}_{\text{IR}}^{(2)} \cdot \hat{\mathbf{d}}_{10}\right)^2 \right] f(\tau),$$

$$\rho_{11}^{(1)}(\tau) = 2 G_{10}^{(1)} G_{10}^{(2)} \left(\mathbf{e}_{\text{IR}}^{(1)} \cdot \hat{\mathbf{d}}_{10}\right) \left(\mathbf{e}_{\text{IR}}^{(2)} \cdot \hat{\mathbf{d}}_{10}\right) f(\tau),$$

$$f(\tau) = \frac{\left| e^{-i(\omega_{\text{IR}} - \omega_{10})\tau} - e^{-\gamma\tau} \right|^2}{(\omega_{\text{IR}} - \omega_{10})^2 + \gamma^2}.$$

A. Polarization dependence of vibrational progression of pump-probe spectra

To avoid cumbersome expressions, until now we considered only the electronic component of the core excitation to

state 2 neglecting the excitation of the vibrational structure in the core-excited (or core-ionized) state. Now we are at the stage to include this vibrational excitation applying Franck-Condon (FC) principle to Eq. (3),

$$\frac{|G_{2n}|^2}{(\omega_X - \omega_{2n})^2 + \Gamma^2} \to |G_{20}|^2 |\mathbf{e}_X \cdot \hat{\mathbf{d}}_{20}|^2 \sigma_n^{\text{nucl}}, \quad n = 0, 1,$$

where

$$\sigma_n^{\text{nucl}} = \sum_\nu \frac{|\langle \nu | n \rangle|^2}{\left[\omega_X - \omega_{20}^{\text{el}} - \left(\epsilon_\nu^{(2)} - \epsilon_n^{(0)} \right) \right]^2 + \Gamma^2}$$

$$= \frac{1}{\Gamma} \operatorname{Re} \int_0^\infty dt \, e^{-i(\omega_{20}^{\text{el}} - \epsilon_n^{(0)} - \omega_X - i\Gamma)t} \langle n | \psi_n^{(c)}(t) \rangle. \quad (6)$$

Here $G_{20} = G_{21} = E_X d_{20}/2$ is the Rabi frequency of electronic transition $0 \to 2$ from the ground to the core-excited state, ω_{20}^{el} is the frequency of electronic transition between bottoms of the potential-energy surfaces of the core-excited and ground states whereas $\epsilon_\nu^{(2)}$ and $\epsilon_n^{(0)}$ are vibrational energies of the core-excited and ground states, respectively, we label the vibrational level of the core-excited state by index ν, and $|\langle \nu | n \rangle|^2$ is the FC factor of core excitation. The nuclear wave-packet $|\psi_n^{(c)}(t)\rangle = e^{-iH_c t}|n\rangle$ is the solution of the time-dependent Schrödinger equation with the nuclear Hamiltonian H_c of the core-excited state [23–25]. Finally, for the absorption profile of the probe x-ray field we obtain

$$\sigma = |G_{20}|^2 |\mathbf{e}_X \cdot \hat{\mathbf{d}}_{20}|^2 \left[\tilde{\sigma} + \rho_{11}^{(1)}(\tau) \left(\sigma_1^{\text{nucl}} - \sigma_0^{\text{nucl}} \right) \cos \varphi \right],$$

$$\tilde{\sigma} = \sigma_0^{\text{nucl}} + \rho_{11}^{(0)} \left(\sigma_1^{\text{nucl}} - \sigma_0^{\text{nucl}} \right). \quad (7)$$

B. $O1s \to 2\pi$ x-ray absorption of CO

As a showcase we selected to study the $X^1\Sigma^+ \to {}^1\Pi(1\sigma^{-1}2\pi^1)$ x-ray absorption of the CO molecule. Calculations of the partial cross-sections σ_0^{nucl} and σ_1^{nucl} were performed using the time-dependent representation [23–25] (6) and potential-energy curves of the ground and core-excited states (Fig. 2) are taken from Refs. [26,27], $\Gamma = 0.079$ eV [27]. The rather large change in the equilibrium bond length under core excitation leads to the rich vibrational structure of conventional XAS σ_0^{nucl} from the lowest vibrational level ($n = 0$) which has a nodeless wave function (Fig. 2). The single node wave function of the pumped vibrational level (Fig. 2) changes qualitatively the FC factors $|\langle \nu | 1 \rangle|^2$ in comparison with $|\langle \nu | 0 \rangle|^2$. This together with the reflection principle [19,28] explain why the envelope of σ_1^{nucl} has a double-peak structure (Fig. 3). Due to strong difference $(\sigma_1^{\text{nucl}} - \sigma_0^{\text{nucl}})$ in the FC distributions (Fig. 3), one can expect a detectable deviation of the IR + x-ray pump-probe spectrum (7) from the conventional XAS from level 0, σ_0^{nucl}. The XAS profiles depicted in Fig. 3 are much wider than the lifetime broadening $\Gamma = 0.079$ eV. The reason for this is the broad vibrational structure which is not fully resolved since the spacing between vibrational levels of the core-excited state (0.177 eV) is comparable with the core-hole lifetime broadening $2\Gamma = 0.158$ eV.

C. Averaging over molecular orientation

In the real situation of the gas-phase or liquid-phase experiment the vibrational progression of x-ray spectra can be
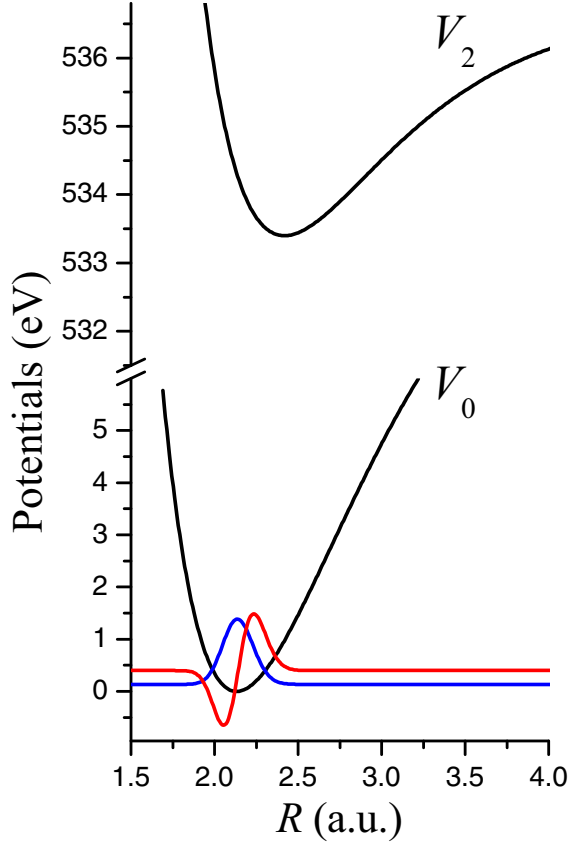
FIG. 2. Potential-energy curves of ground $X^1\Sigma^+$ (V_0) and core-excited $O1s^{-1}2\pi^1$ (V_2) states of the CO molecule. Solid blue and red lines display the vibrational wave-functions $|0\rangle$ and $|1\rangle$, respectively.

affected by the random molecular orientation. To study this problem in more detail let us write down the expression for the probe XAS and x-ray photoionization spectra averaged over molecular orientations.

1. X-ray absorption

First let us consider the x-ray absorption of molecules pumped by the IR field. In the case of randomly oriented molecules we should average the cross section over molecular orientation using the following equations [6]:

$$\overline{\hat{d}_i\hat{d}_j} = \frac{1}{3}\delta_{ij},$$

$$\overline{\hat{d}_i\hat{d}_j\hat{D}_k\hat{D}_l} = \frac{1}{15}\{\delta_{ij}\delta_{kl}(2 - \cos^2\chi)$$
$$+ \frac{1}{2}(\delta_{ik}\delta_{jl} + \delta_{il}\delta_{jk})(3\cos^2\chi - 1)\}. \quad (8)$$

Here $\chi = \angle(\mathbf{d}, \mathbf{D}) = \angle(\mathbf{d}_{10}, \mathbf{d}_{20})$, $\hat{d}_i$, and $\hat{D}_i$ are the Cartesian coordinates of $\hat{\mathbf{d}} = \hat{\mathbf{d}}_{10}$ and $\hat{\mathbf{D}} = \hat{\mathbf{d}}_{20}$. Applying Eq. (8) to Eq. (7) we get the following XAS cross section for randomly oriented molecules:

$$\sigma_{\text{XAS}} = \frac{|G_{20}|^2}{3}\left\{\sigma_0^{\text{nucl}} + \frac{\kappa}{5}(\sigma_1^{\text{nucl}} - \sigma_0^{\text{nucl}})P_{\text{XAS}}\right\}, \quad (9)$$

where the dimensionless saturation parameter,

$$\kappa = \left[\left(G_{10}^{(1)}\right)^2 + \left(G_{10}^{(2)}\right)^2\right]f(\tau)$$

characterizes the population $\rho_{11}(\tau)$ (2) of the excited vibrational level by the IR pulse. It can be shown, that the averaging over molecular orientation (e.g., orientation of the electronic transition dipole moments) in the laboratory frame with the help of Eq. (8) results in the following equation for the polarization function:

$$P_{\text{XAS}} = 2 - \cos^2\chi + (3\cos^2\chi - 1)\left[\xi_1^2\left(\mathbf{e}_{\text{IR}}^{(1)} \cdot \mathbf{e}_X\right)^2 + \xi_2^2\left(\mathbf{e}_{\text{IR}}^{(2)} \cdot \mathbf{e}_X\right)^2\right]$$
$$+ 2\xi_1\xi_2\left[(2 - \cos^2\chi)\left(\mathbf{e}_{\text{IR}}^{(1)} \cdot \mathbf{e}_{\text{IR}}^{(2)}\right) + (3\cos^2\chi - 1)\left(\mathbf{e}_{\text{IR}}^{(1)} \cdot \mathbf{e}_X\right)\left(\mathbf{e}_{\text{IR}}^{(2)} \cdot \mathbf{e}_X\right)\right]\cos\varphi,$$
$$\xi_n = \frac{E_n}{\sqrt{E_1^2 + E_2^2}}, \quad n = 0, 1 \quad (10)$$

depends on the angle between transition dipole moments of the IR and the x-ray transitions $\chi = \angle(\mathbf{d}_{10}, \mathbf{d}_{20}) = \angle(\mathbf{R}, \mathbf{d}_{20})$ and the mutual orientation of the polarization vectors of the IR field $\mathbf{e}_{\text{IR}}^{(1)}$, $\mathbf{e}_{\text{IR}}^{(2)}$, and of the x-ray pulse $\mathbf{e}_X$. Let us consider a rather common case when all the polarization vectors are lying on the same plane,

$$P_{\text{XAS}} \equiv P_{\text{XAS}}(\beta_1, \beta_2) = 2 - \cos^2\chi + (3\cos^2\chi - 1)$$
$$\times \left(\xi_1^2\cos^2\beta_1 + \xi_2^2\cos^2\beta_2\right)$$
$$+ 2\xi_1\xi_2[(2 - \cos^2\chi)\cos(\beta_2 - \beta_1)$$
$$+ (3\cos^2\chi - 1)\cos\beta_1\cos\beta_2]\cos\varphi, \quad (11)$$

where $\beta_1 = \angle(\mathbf{e}_{\text{IR}}^{(1)}, \mathbf{e}_X)$ and $\beta_2 = \angle(\mathbf{e}_{\text{IR}}^{(2)}, \mathbf{e}_X)$. The polarization function of the pump-probe XAS depends also on the angle χ between the transition dipole moments of the IR and

x-ray transitions, which is equal to 0 and $\pi/2$ for $1s \to \sigma^*$ and for $1s \to \pi^*$ core excitations in diatomic molecules. Figures 4 and 5 display the strong dependence of $P_{\text{XAS}}(\beta_1, \beta_2)$ on β_1 and β_2 which is qualitatively different for σ^* and π^* core excitations.

In the simplest but physically important case, $\xi_1 = \xi_2 = 1/\sqrt{2}$, $\beta_1 = \beta_2 \equiv \beta$ the polarization function (8) becomes

$$P_{\text{XAS}} = [2 - \cos^2\chi + (3\cos^2\chi - 1)\cos^2\beta](1 + \cos\varphi).$$

This function is equal to zero when $\varphi = \pi$ simply because $|\mathbf{E}_{\text{IR}}|^2 = 0$ and, hence, vibrational level 1 is not populated, $\rho_{11} \propto |G_{10}|^2 \propto |\mathbf{E}_{\text{IR}}|^2 = 0$. In the case of $1s \to \sigma^*$ XAS ($\chi = 0$) the polarization function $P_{\text{XAS}} = (1 + 2\cos^2\beta)(1 + \cos\varphi)$ takes a maximum $P_{\text{XAS}} = 6$ when $\beta = 0, \pi$ and its minimum value $P_{\text{XAS}} = 2$ when $\beta = \pi/2$ ($\varphi = 0$). This is
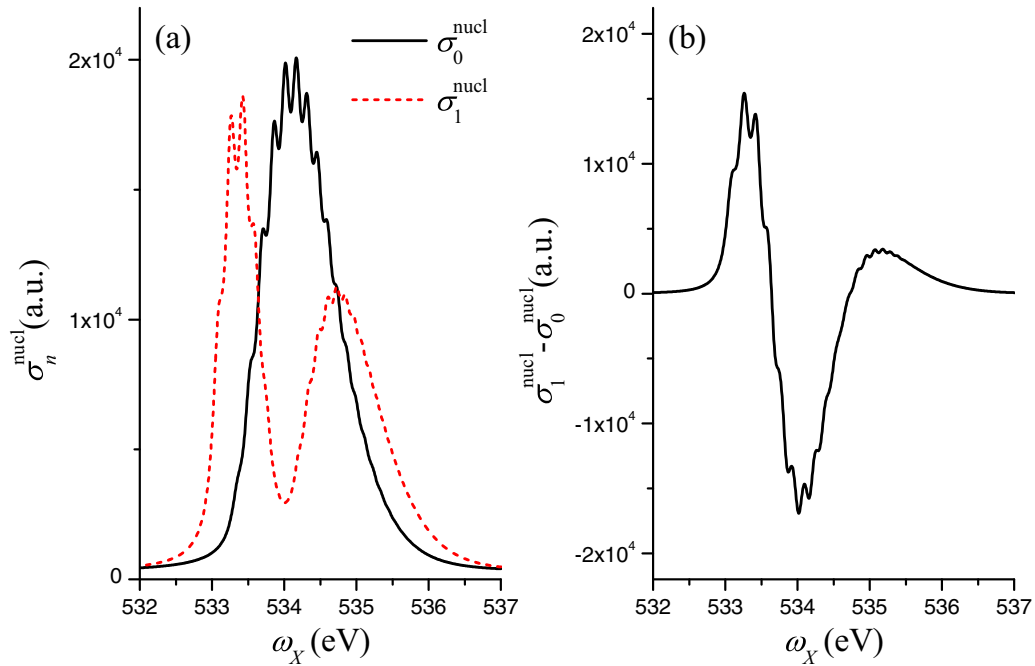
FIG. 3. (a) X-ray absorption $X^1\Sigma^+ \to O1s^{-1}2\pi^1$ of CO from the lowest σ_0^{nucl} (black solid line) and pumped σ_1^{nucl} (dashed red line) vibrational levels. (b) The difference of the FC distributions of the XAS from panel (a) $\sigma_1^{\mathrm{nucl}} - \sigma_0^{\mathrm{nucl}}$. $\Gamma = 0.079$ eV.

because the x-ray transition $1 \to 2$ from the pumped vibrational level occurs preferentially from molecules aligned along the polarization vector of the IR field $\mathbf{e}_{\mathrm{IR}}^{(n)}$, inasmuch as the probability of pump IR transition $\propto (\mathbf{e}_{\mathrm{IR}}^{(n)} \cdot \mathbf{d}_{10})^2$ takes a maximum when the molecular axis is parallel to $\mathbf{e}_{\mathrm{IR}}^{(n)}$. The picture is opposite for the $1s \to \pi^*$ core-excitation ($\chi = \pi/2$) with $P_{\mathrm{XAS}} = (2 - \cos^2 \beta)(1 + \cos \varphi)$ since now $\mathbf{d}_{20} \perp \mathbf{R}$, P_{XAS} is maximal when polarization vectors of IR and x-ray fields are orthogonal $\beta = \pi/2$. This effect has close analogy with the polarization anisotropy of RIXS [5,6].

2. X-ray-induced core ionization

In the case of core-ionization (x-ray photoemission spectra) we should perform the following replacement in σ_n^{nucl} [see Eq. (6)],

$$\omega_X - \omega_{20}^{\mathrm{el}} \to \mathrm{BE} - I,$$

where $\mathrm{BE} = \omega_X - \varepsilon$ is the binding energy, I is the ionization potential of core electron, and ε is the energy of photoelectron. The polarization dependence of the photoionization at the molecular K edge differs qualitatively from the one
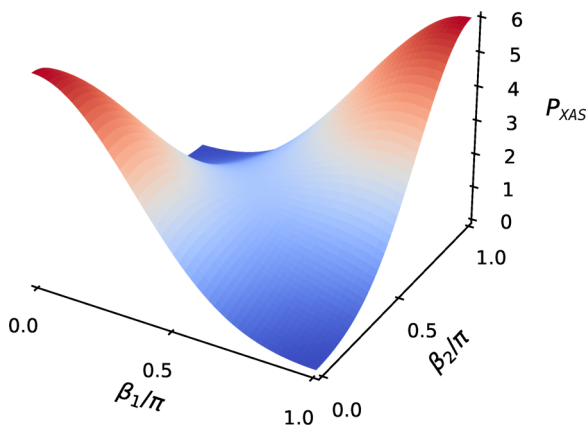
FIG. 4. Polarization function $P(\beta_1, \beta_2)$ for $1s \to \sigma^*$ pump-probe XAS (8). $\chi = 0$, $\xi_1 = \xi_2 = 1/\sqrt{2}$, $\varphi = 0$. $P_{\mathrm{XAS}}(\beta_1, \beta_2)$ is symmetric with respect to reflection relative to the diagonals $(0, 0) - (1, 1)$ and $(1, 0) - (0, 1)$.
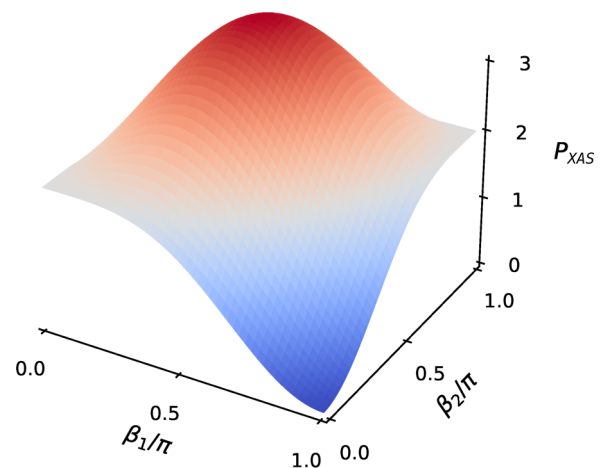
FIG. 5. Polarization function $P_{\mathrm{XAS}}(\beta_1, \beta_2)$ for $1s \to \pi^*$ pump-probe XAS (8). $\chi = \pi/2$, $\xi_1 = \xi_2 = 1/\sqrt{2}$, $\varphi = 0$. $P_{\mathrm{XAS}}(\beta_1, \beta_2)$ is symmetric with respect to reflection relative to the diagonals $(0, 0) - (1, 1)$ and $(1, 0) - (0, 1)$.
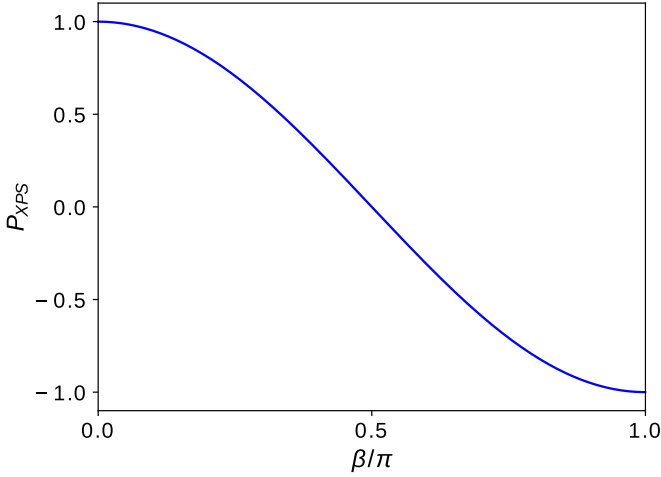
FIG. 6. Polarization function $P_{\mathrm{XPS}}(\beta)$ of pump-probe XPS (10). $\beta = \angle(\mathbf{e}_1^{(1)}, \mathbf{e}_1^{(2)})$, $\xi_1 = \xi_2 = 1/\sqrt{2}$, $\varphi = 0$.

of x-ray absorption because the transition dipole moment of the $1s$ ionization is parallel to the momentum of the photoelectron $\mathbf{k}$,

$$\hat{\mathbf{d}}_{20} = \hat{\mathbf{k}}.$$

Due to this the orientational averaging is performed using only the upper equation in (8), which results in the following form of the XPS cross section,

$$\sigma_{\mathrm{XPS}} = |G_{20}|^2 (\mathbf{e}_X \cdot \hat{\mathbf{k}})^2$$
$$\times \left\{ \sigma_0^{\mathrm{nucl}} + \frac{\kappa}{3}(1 + P_{\mathrm{XPS}})\left(\sigma_1^{\mathrm{nucl}} - \sigma_0^{\mathrm{nucl}}\right) \right\}. \quad (12)$$

Since $\hat{\mathbf{d}}_{20} = \hat{\mathbf{k}}$ there is no correlation between the polarization vectors of x-ray ($\mathbf{e}_X$) and IR ($\mathbf{e}_{\mathrm{IR}}^{(n)}$) fields. Therefore, the polarization function depends only on angle between the polarizations of the two IR fields $\mathbf{e}_{\mathrm{IR}}^{(1)}$ and $\mathbf{e}_{\mathrm{IR}}^{(2)}$ but not on the orientation of the x-ray polarization vector,

$$P_{\mathrm{XPS}} \equiv P_{\mathrm{XPS}}(\beta) = 2\xi_1\xi_2(\mathbf{e}_{\mathrm{IR}}^{(1)} \cdot \mathbf{e}_{\mathrm{IR}}^{(2)})\cos\varphi$$
$$= 2\xi_1\xi_2 \cos\varphi \cos\beta, \quad (13)$$

where $\beta = \angle(\mathbf{e}_{\mathrm{IR}}^{(1)}, \mathbf{e}_{\mathrm{IR}}^{(2)})$. Figure 6 illustrates the function $P_{\mathrm{XPS}}(\beta)$ which has a rather strong dependence on the relative orientation of the polarization vectors of the IR fields.

D. Extraction of $\sigma_1^{\mathrm{nucl}} - \sigma_0^{\mathrm{nucl}}$ from pump-probe measurements

Let us discuss now how the polarization effects can be used for extraction of the partial XAS and XPS cross sections originating from the ground and excited vibrational levels σ_1^{nucl} and σ_0^{nucl}, respectively. Indeed, in a real experiment it is rather difficult to populate significantly the excited vibrational level $n = 1$ and, thus, to measure separately the σ_1^{nucl} profile in order to get the difference of FC distributions for excitation from excited and lowest vibrational states $\sigma_1^{\mathrm{nucl}} - \sigma_0^{\mathrm{nucl}}$. However, the polarization dependence of IR-pump, XAS-, and XPS-probe techniques proposed above allows to extract the spectral distribution of a weak $(\sigma_1^{\mathrm{nucl}} - \sigma_0^{\mathrm{nucl}})$ contribution directly from the experiment. In order to show this, let us first normalize the XAS and XPS cross sections on the area of the vibrational profile. With the help of identity $\int \sigma_n^{\mathrm{nucl}} d\omega = \pi/\Gamma$

we get the following expressions for the areas of the XAS (9) and XPS (12) vibrational bands,

$$S_{\mathrm{XAS}} = \int_{-\infty}^{\infty} \sigma_{\mathrm{XAS}} d\omega = \frac{\pi}{3\Gamma}|G_{20}|^2,$$

$$S_{\mathrm{XPS}} = \int_{-\infty}^{\infty} \sigma_{\mathrm{XPS}} d\varepsilon = \frac{\pi}{\Gamma}|G_{20}|^2(\mathbf{e}_X \cdot \hat{\mathbf{k}})^2,$$

and the normalized XAS ($\tilde{\sigma}_{\mathrm{XAS}} = \sigma_{\mathrm{XAS}}/S_{\mathrm{XAS}}$) and XPS ($\tilde{\sigma}_{\mathrm{XPS}} = \sigma_{\mathrm{XPS}}/S_{\mathrm{XPS}}$) cross sections read

$$\tilde{\sigma}_{\mathrm{XAS}} = \frac{\Gamma}{\pi}\left\{ \sigma_0^{\mathrm{nucl}} + \frac{\kappa}{5}\left(\sigma_1^{\mathrm{nucl}} - \sigma_0^{\mathrm{nucl}}\right)P_{\mathrm{XAS}} \right\},$$

$$\tilde{\sigma}_{\mathrm{XPS}} = \frac{\Gamma}{\pi}\left\{ \sigma_0^{\mathrm{nucl}} + \frac{\kappa}{3}(1 + P_{\mathrm{XPS}}\cos\varphi)\left(\sigma_1^{\mathrm{nucl}} - \sigma_0^{\mathrm{nucl}}\right) \right\}.$$

The structure of the above equations is very clear: the first term σ_0^{nucl} describes the conventional XAS and XPS signals when the IR field is turned off, whereas the second term proportional to κ arises fully from the IR-pump effect. Only the second term shows dependence on the polarization and, thus, can be used to extract the FC difference we are looking for. Indeed, the small pump-probe signal contribution $\propto \kappa(\sigma_1^{\mathrm{nucl}} - \sigma_0^{\mathrm{nucl}})$ is accessible by a subtraction of the cross section obtained for another values of the polarization functions P_{XAS} and P_{XPS}, which cancels out the major one-photon $0 \rightarrow 2$ contribution σ_0^{nucl},

$$\tilde{\sigma}'_{\mathrm{XAS}} - \tilde{\sigma}_{\mathrm{XAS}} = \frac{\Gamma\kappa}{5\pi}(P'_{\mathrm{XAS}} - P_{\mathrm{XAS}})\left(\sigma_1^{\mathrm{nucl}} - \sigma_0^{\mathrm{nucl}}\right),$$

$$\tilde{\sigma}'_{\mathrm{XPS}} - \tilde{\sigma}_{\mathrm{XPS}} = \frac{\Gamma\kappa}{3\pi}(P'_{\mathrm{XPS}} - P_{\mathrm{XPS}})\left(\sigma_1^{\mathrm{nucl}} - \sigma_0^{\mathrm{nucl}}\right). \quad (14)$$

Here P_{XAS} and P'_{XAS} (P_{XPS} and P'_{XPS}) correspond to the measurements with the two sets of polarization vectors angles $P_{\mathrm{XAS}} \equiv P_{\mathrm{XAS}}(\beta_1, \beta_2)$ and $P'_{\mathrm{XAS}} \equiv P_{\mathrm{XAS}}(\beta'_1, \beta'_2)$ [$P_{\mathrm{XPS}} \equiv P_{\mathrm{XPS}}(\beta)$ and $P'_{\mathrm{XPS}} \equiv P_{\mathrm{XPS}}(\beta')$], respectively. Using the shape of the polarization functions, depicted in Figs. 4–6, one can maximize the pump-probe signal in (. For example, the polarization function for XAS on the $1s \rightarrow \sigma^*$ transition reaches its maximal value of $P_{\mathrm{XAS}}^{\mathrm{max}} = 6.0$ when the polarization vectors of both IR pulses are parallel (antiparallel) to the x-ray polarization, and it is at the saddle-point $P_{\mathrm{XAS}} = 3.0$ when IR and x-ray polarizations are orthogonal $\beta_1 = \beta_2 = \pi/2$. These two sets of polarization angles can be easily fixed in the experiment. Similarly, the optimal polarization vectors ansatz can be defined for the case of XAS on the $1s \rightarrow \pi^*$ transition (Fig. 5) and XPS measurements (Fig. 6).

It is worthwhile to note that the proposed experimental scheme can be realized using a split-delay-merge unit for IR laser pulses with variable polarization with respect to x rays and a general delay unit to scan the time difference between IR and x-ray pulses. In that case, independent control of the polarization, phase shift, and delay can be achieved. We believe, that present day instrumental development allows to inspect the validity of our theoretical results in the real experimental situation. Equipment for XAS and XPS measurements is available at many synchrotron beamlines.

E. Role of molecular rotation

The x-ray spectra can be affected also by rotational degrees of freedom [29,30], which were, so far, neglected in our theoretical description. This approximation is valid when the time-delay Δt between the IR and the x-ray pulses is shorter than the period of rotation $2\pi/\omega_{\text{rot}}$. However, the rotation has to be taken into account [29] when $\omega_{\text{rot}}\Delta t > 1$. The effect of rotation can be also observed with the help of the proposed pump-probe technique, and, thus, let us discuss this effect qualitatively.

Molecular rotation affects the angle

$$\chi = \cos^{-1}(\hat{\mathbf{d}}_{10} \cdot \hat{\mathbf{d}}_{20}) \rightarrow \chi(\Delta t) = \cos^{-1}[\hat{\mathbf{d}}_{10} \cdot \hat{\mathbf{d}}_{20}(\Delta t)],$$

between the transition dipole moments of IR ($\mathbf{d}_{10}$) and x-ray absorption ($\mathbf{d}_{20}$) transitions because the molecule changes the orientation during the time delay,

$$\chi(\Delta t) = \chi(0) + \omega_{\text{rot}}\Delta t. \tag{15}$$

Let us consider the simple case of diatomic molecules where $\hat{\mathbf{d}}_{10}$ is parallel to the molecular axis $\mathbf{R}$: $\hat{\mathbf{d}}_{10} = \hat{\mathbf{R}}$. The angle χ depends on the symmetry of the core-excited state: $\chi = 0$ or $\pi/2$ for the $1s \rightarrow \sigma^*$ or $1s \rightarrow \pi^*$ transitions, respectively. The molecular rotation affects the polarization function (10) via the change in the angle $\chi(\Delta t)$ (11) from its initial value $\chi(0) = 0$ for the $1s \rightarrow \sigma^*$ and $\chi(0) = \pi/2$ for the $1s \rightarrow \pi^*$ XAS transitions. The variation of the polarization function (10) $P_{\text{XAS}} \rightarrow P_{\text{XAS}}(\Delta t)$ with the change in the delay time between probe x-ray and pump IR pulses,

$$\sigma^*: \cos^2\chi(\Delta t) = \cos^2(\omega_{\text{rot}}\Delta t) = \frac{1 + \cos(2\omega_{\text{rot}}\Delta t)}{2},$$

$$\pi^*: \cos^2\chi(\Delta t) = \sin^2(\omega_{\text{rot}}\Delta t) = \frac{1 - \cos(2\omega_{\text{rot}}\Delta t)}{2}$$

affects also the whole shape of the XAS profile. This together with the polarization sensitivity of the pump-probe technique introduced above gives an additional tool to study the rotational dynamics of free molecules and liquids. Contrary to x-ray absorption, the polarization anisotropy of the core ionization at the K edge shows no sensitivity to the molecular rotation since the $1s$ ionization does not depend on the angle χ [see Eq. (10)]. This effect in pump-probe XAS spectra can be used for investigations of the dynamics of phase transitions in liquids and solids [31] on a large variation scale of Δt from femtoseconds to pico- and nanoseconds.

Evidently, the thermal motion reduces the oscillations $\cos(2\omega_{\text{rot}}\Delta t)$. Let us evaluate this damping treating rotations classically. For diatomic molecules, there are two independent rotations with angular velocities $\boldsymbol{\omega}_x$ and $\boldsymbol{\omega}_y$ orthogonal to molecular axis $\mathbf{R}$. In the classical picture the molecules rotate with total angular velocity $\boldsymbol{\omega}_{\text{rot}} = \boldsymbol{\omega}_{\text{rot}}^{(x)} + \boldsymbol{\omega}_{\text{rot}}^{(y)}$ [$\omega_{\text{rot}} = \sqrt{(\omega_{\text{rot}}^{(x)})^2 + (\omega_{\text{rot}}^{(y)})^2}$]. We need the following expectation value (see Appendix B),

$$\overline{\cos(2\omega_{\text{rot}}\Delta t)}$$

$$= \text{Re} \int_{-\infty}^{\infty} d\omega_{\text{rot}}^{(x)} \int_{-\infty}^{\infty} d\omega_{\text{rot}}^{(y)} e^{i2\omega_{\text{rot}}\Delta t} W\left(\omega_{\text{rot}}^{(x)}\right) W\left(\omega_{\text{rot}}^{(y)}\right)$$

$$= C(\bar{\omega}\,\Delta t), \quad C(\eta) = 1 - 2\eta e^{-\eta^2} \int_0^{\eta} e^{x^2} dx. \tag{16}$$
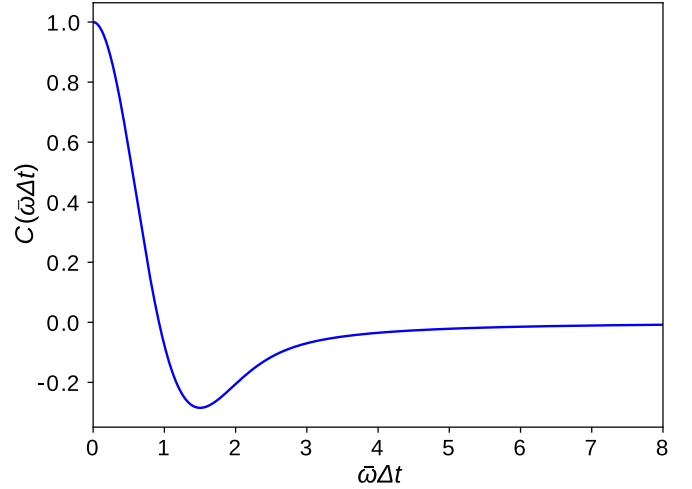
FIG. 7. Function $C(\bar{\omega}\,\Delta t)$ (12) shows the damping of the rotational modulation $\cos(2\omega_{\text{rot}}\Delta t)$ because of thermal rotational motion. $C(\bar{\omega}\,\Delta t)$ takes a minimum at $\bar{\omega}\,\Delta t = 1.5$. For the CO molecule at room temperature $\bar{\omega} \approx 1.87 \times 10^{-4}$ a.u. This corresponds to $\Delta t = 1.5/\bar{\omega} \approx 194$ fs.

Here $W(\omega) = (1/\sqrt{\pi}\bar{\omega}) \exp(-\omega^2/\bar{\omega}^2)$ is the one-dimensional Maxwell-Boltzmann distribution over rotational frequencies $\bar{\omega} = \sqrt{2k_B T/I}$ is the thermal angular velocity for the temperature T, $I = \mu R^2$ is the moment of inertia, and μ is the reduced mass. Figure 7 shows that the thermal rotational motion quenches the oscillations, and only first bend of $\cos(2\omega_{\text{rot}}\Delta t)$ survives. To make the oscillations caused by molecular rotation more pronounced it is necessary to create a nonequilibrium rotational distribution (alignment or orientation) [32,33]. One of the well-known ways to produce unidirectional rotation is to use a circularly polarized pump laser field $\mathbf{e}_\pm = \mathbf{e}_x \pm i\mathbf{e}_y$,

$$\langle J_0 M_0|(\mathbf{e}_\pm \cdot \hat{\mathbf{R}})|JM\rangle, \quad M = M_0 \pm 1, \tag{17}$$

which can create significant orientation of angular velocities parallel to $\mathbf{e}_\pm$. A very efficient technique to create a unidirectionally rotating wave packet is the "optical centrifuge" using the gradually accelerating circularly rotating laser polarization field [34]. The pulse chirp provides a complementary method of shaping and probing of the rotational wave packet in the ground electronic state [35,36] as well as the vibrational wave packet [37,38].

IV. SUMMARY

We proposed an IR-x-ray pump-probe scheme which utilizes two time-delayed coherent IR pulses with controlled polarization direction as the pump. As the probe we study the possibility of using x-ray absorption and x-ray photoelectron spectroscopy. With the help of theoretical analysis we have found a strong polarization sensitivity with respect to relative orientation of the polarization vectors of the two IR-pump and x-ray-probe fields. Moreover, we demonstrated that the polarization-resolved measurements can be used as a reliable method to extract directly from the experiment the difference between the Franck-Condon progressions from the lowest and the first excited vibrational levels of the ground electronic

state. Our findings are exemplified for $O1s \rightarrow 2\pi$ x-ray absorption of the CO molecule pumped by two coherent IR pulses. We discussed possible experimental conditions which allow to maximize the observed effect by particular relative alignment of the polarization vectors of the three electromagnetic pulses.

The proposed pump-probe scheme suggests a promising protocol for delicate control of IR-induced nuclear dynamics probed in x-ray absorption and ionization spectra. This scheme has a number of advantages, which makes it attractive for experimental application. In particular, there is no need for strong IR and x-ray fields, no special requirements on pulse duration, and the delay time between the pump and the probe pulses can be varied in a broad interval. All this makes it possible to apply the pump-probe techniques even at synchrotron radiation facility where a variety of x-ray pulse durations can be reached with the help of the electron bunch slicing technique.

The possibility to study effects of molecular rotation is presented qualitatively through variations in the delay time between the pump and the probe pulses. Since in our method the time delay is not limited, the proposed method becomes potentially very attractive for the study of the photoinduced phase transitions in liquids and solids. The outlined probe-field spectroscopy is not limited to XAS and XPS and can be in extended to other more sophisticated schemes, for example, by using RIXS spectroscopy as a probe.

APPENDIX A: INTERFERENCE OF ONE- AND TWO-PHOTON CHANNELS

The interference between one- and two-photon channels x-ray absorption or core-ionization channels (4) experiences beating with the frequency of the vibrational transitions $e^{-i\omega_{10}t}$. Since the experimental setup integrates the cross section over the x-ray pulse, the interference term $\propto e^{-i\omega_{10}t} = e^{-i\omega_{10}(t-t_X)}e^{-i\omega_{10}t_X}$ should be averaged over the x-ray pulse as well [14,15]. For example, the Gaussian x-ray pulse results in the following expression:

$$G_{21}G_{20}^* e^{-i\omega_{10}t} \rightarrow e^{-i\omega_{10}t_X} \langle G_{21}G_{20}^* e^{-i\omega_{10}(t-t_X)} \rangle$$
$$\approx G_{21}G_{20}^* \zeta e^{-i\omega_{10}t_X},$$
$$\zeta = \langle e^{-i\omega_{10}(t-t_X)} \rangle$$

$$\approx \int_{-\infty}^{\infty} dt \, e^{-i\omega_{10}t} \frac{\exp[-(t/\tau_X)^2]}{\tau_X\sqrt{\pi}}$$
$$= \exp[-(\omega_{10}\tau_X/2)^2],$$

$\tau_X = \tau_X^{\text{HWHM}}/\sqrt{\ln 2}$ is the duration of the x-ray pulse. Thus, the interference contribution (4) is suppressed for x-ray pulse longer than the period of molecular vibrations $\tau_X\omega_{10} \gg 1$. This interference becomes important for short x-ray pulses $\tau_X\omega_{10} \lesssim 1$ [14,15,39]. But in this case we lose the vibrational resolution [14,15] required for distinguishing between $1 \rightarrow 2$ and $0 \rightarrow 2$ transitions.

One should note that the factor $e^{-i\omega_{10}t} \rightarrow 1$ and the related suppression of the interference term will be absent in the case of the coherent two-color x-ray pulse [40] with two frequencies ω and ω' satisfying the condition $\omega' - \omega = \omega_{10}$. Indeed, the one- and two-photon absorption (or ionization) channels lead to the same energy of the final state,

$$\omega' + E_0 = \omega + \omega_{\text{IR}} + E_0.$$

There is yet another reason for suppression of coherent term σ_{coh}. The discussed interference is very sensitive to averaging of the cross section over molecular orientation [14,15],

$$\sigma_{\text{coh}} \propto \overline{(\mathbf{E}_{\text{IR}} \cdot \mathbf{d}_{10})|\mathbf{E}_X \cdot \mathbf{d}_{20}|^2}.$$

Apparently this term is equal to zero for randomly oriented molecules in gas or liquid phases because $\overline{(\mathbf{E}_{\text{IR}} \cdot \mathbf{d}_{10})}x = 0$. However, the interference of one- and two-photon channels becomes important for surface adsorbed molecules. Indeed, quite often the adsorbed molecules have preferential orientation [41–44]. One should note that the molecules can be oriented even in the gas phase by a laser field [32,33]. The interference term σ_{coh} (4) was studied earlier [14,15], and it is neglected in the present paper.

APPENDIX B: SUPPRESSION OF cos OSCILLATIONS BY THERMAL MOTION

Using the cylindrical symmetry of the integrand in Eq. (12) lets us go from Cartesian to cylindrical coordinates $\iint d\omega_{\text{rot}}^{(x)} d\omega_{\text{rot}}^{(y)} = 2\pi \int \omega_{\text{rot}} d\omega_{\text{rot}}$,

$$\overline{\cos(2\omega_{\text{rot}}t)} = \frac{1}{\pi\bar{\omega}^2}\text{Re}\int_{-\infty}^{\infty} d\omega_{\text{rot}}^{(x)} \int_{-\infty}^{\infty} d\omega_{\text{rot}}^{(y)} e^{i2\omega_{\text{rot}}t} e^{-\omega_{\text{rot}}^2/\bar{\omega}^2}$$
$$= \frac{2}{\bar{\omega}^2}\text{Re}\int_0^{\infty} d\omega_{\text{rot}}\omega_{\text{rot}}e^{i2\omega_{\text{rot}}t} e^{-\omega_{\text{rot}}^2/\bar{\omega}^2}$$
$$= \frac{1}{\bar{\omega}}\frac{\partial}{\partial t}\left\{e^{-(\bar{\omega}t)^2}\int_0^{\bar{\omega}t} d\eta \, e^{\eta^2}\right\}$$
$$= C(\bar{\omega}t),$$

where

$$C(x) = 1 - 2xe^{-x^2}\int_0^x d\eta \, e^{\eta^2} = 1 - \sqrt{\pi}xe^{-x^2}\text{erfi}(x).$$

Here $\text{erfi}(x)$ is the imaginary error function.

[1] M. Drescher, M. Henschel, R. Klenberger *et al.*, Time-resolved atomic inner-shell spectroscopy, Nature (London) **419**, 803 (2002).

[2] C. Bressler nd M. Chergui, Ultrafast X-ray absorption spectroscopy, Chem. Rev. **104**, 1781 (2004).

[3] M. Beye, F. Sorgenfrei, W. F. Schlotter, W. Wurth, and A. Föhlisch, The liquid-liquid phase transition in silicon revealed by snapshots of valence electrons, Proc. Natl. Acad. Sci. USA **107**, 16772 (2010).

[4] H.-S. Tan, I. R. Piletic, and M. D. Fayer, Polarization selective spectroscopy experiments: Methodology and pitfalls, J. Opt. Soc. Am. B **22**, 2009 (2005).

[5] F. Gel'mukhanov and L. N. Mazalov, Polarisation of the X-ray fluorescence of molecules, Opt. Spektrosk. **42**, 659 (1977) [Opt. Spectrosc. (USSR) **42**, 371 (1977)].

[6] F. Gel'mukhanov and H. Ågren, Resonant inelastic x-ray scattering with symmetry-selective excitation, Phys. Rev. A **49**, 4378 (1994).

[7] S. H. Southworth, Resonance and threshold effects in polarized X-ray emission from atoms and molecules, Nucl. Instrum. Methods Phys. Res., Sect. B **87**, 247 (1994).

[8] F. Gel'mukhanov and H. Ågren, Resonant X-ray Raman scattering, Phys. Rep. **312**, 87 (1999).

[9] X. Gao, D. Casa, J. Kim, T. Gog, C. Li, and C. Burns, Toroidal silicon polarization analyzer for resonant inelastic X-ray scattering, Rev. Sci. Instrum. **87**, 083107 (2016).

[10] C. Buth, R. Santra, and L. Young, Electromagnetically Induced Transparency for X-rays, Phys. Rev. Lett. **98**, 253001 (2007).

[11] E. R. Peterson, C. Buth, D. A. Arms, R. W. Dunford, E. P. Kanter, B. Krässig, E. C. Landahl, S. T. Pratt, R. Santra, S. H. Southworth, and L. Young, Appl. Phys. Lett. **92**, 094106 (2008).

[12] J.-C. Liu, Y. Velkov, Z. Rinkevicius, H. Ågren, and F. Gel'mukhanov, Symmetry-forbidden X-ray Raman scattering induced by a strong infrared-laser field, Symmetry-forbidden x-ray Raman scattering induced by a strong infrared-laser field, Phys. Rev. A **77**, 043405 (2008).

[13] L. Young, C. Buth, R. W. Dunford, P. Ho, E. P. Kanter, B. Krässig, E. R. Peterson, N. Rohringer, R. Santra, and S. H. Southworth, Using strong electromagnetic fields to control X-ray processes, Rev. Mex. Fís. S **56**, 11 (2010).

[14] F. F. Guimarães, V. Kimberg, F. Gel'mukhanov, A. Cesar, and H. Ågren, Two-color phase sensitive X-ray pump-probe spectroscopy, Phys. Rev. A **70**, 062504 (2004).

[15] F. F. Guimarães, V. Kimberg, V. C. Felicíssimo, F. Gel'mukhanov, A. Cesar, and H. Ågren, Infrared-x-ray pump-probe spectroscopy of the NO molecule, Phys. Rev. A **72**, 012714 (2005).

[16] V. C. Felicíssimo, F. F. Guimarães, and F. Gel'mukhanov, Enhancement of the recoil effect in X-ray photoelectron spectra of molecules driven by a strong IR field, Phys. Rev. A **72**, 023414 (2005).

[17] F. F. Guimarães and F. Gel'mukhanov, Pump-probe spectroscopy of molecules driven by infrared field in both ground and excited electronic states, J. Chem. Phys. **125**, 204313 (2006).

[18] N. Ignatova, V. Vaz da Cruz, R. C. Couto, E. Ertan, A. Zimin, F. F. Guimarães, S. Polyutov, H. Ågren, V. Kimberg, M. Odelius, and F. Gel'mukhanov, Gradual collapse of nuclear

[19] N. Ignatova, V. Vaz da Cruz, R. C. Couto, E. Ertan, M. Odelius, H. Ågren, F. F. Guimarães, A. Zimin, S. P. Polyutov, F. Gel'mukhanov, and V. Kimberg, Infrared-pump-X-ray-probe spectroscopy of vibrationally excited molecules, Phys. Rev. A **95**, 042502 (2017).

[20] N. Saito, H. Sannohe, N. Ishii, T. Kanai, N. Kosugi, Y. Wu, A. Chew, S. Han, Z. Chang, J. Itatani, Real-time observation of electronic, vibrational, and rotational dynamics in nitric oxide with attosecond soft X-ray pulses at 400 eV, Optica **6**, 1542 (2019).

[21] Y. Pertot, C. Schmidt, M. Matthews, A. Chauvet, M. Huppert, V. Svoboda, A. Von Conta, A. Tehlar, D. Baykusheva, J. P. Wolf, and H. J. Wörner, Time-resolved X-ray absorption spectroscopy with a water window high-harmonic source, Science **355**, 264 (2017).

[22] M. Drabbels and A. M. Wodtke, The determination of the infrared radiative lifetimes of a vibrationally excited neutral molecule using stimulated-emission-pumping, molecular-beam time-of-flight, J. Chem. Phys. **106**, 3024 (1997).

[23] R. C. Couto, V. Vaz da Cruz, E. Ertan, S. Eckert, M. Fondell, M. Dantz, B. Kennedy, T. Schmitt, A. Pietzsch, F. F. Guimarães, H. Ågren, F. Gel'mukhanov, M. Odelius, V. Kimberg, and A. Föhlisch, Selective gating to vibrational modes through resonant X-ray scattering, Nat. Commun. **8**, 14165 (2017).

[24] V. Vaz da Cruz, F. Gel'mukhanov, S. Eckert, M. Iannuzzi, E. Ertan, A. Pietzsch, R. C. Couto, J. Niskanen, M. Fondell, M. Dantz, T. Schmitt, X. Lu, D. McNally, R. M. Jay, Vi. Kimberg, A. Föhlisch, and M. Odelius, Probing hydrogen bond strength in liquid water by resonant inelastic X-ray scattering, Nat. Commun. **10**, 1013 (2019).

[25] V. Vaz da Cruz, N. Ignatova, R. C. Couto, D. Fedotov, D. R. Rehn, V. Savchenko, P. Norman, S. Polyutov, J. Niskanen, S. Eckert, R. M. Jay, M. Fondel, T. Schmidt, A. Pietzsch, A. Föhlich, F. Gel'mukhanov, M. Odelius, and V. Kimberg, Nuclear dynamics in resonant inelastic X-ray scattering and X-ray absorption of methanol, J. Chem. Phys. **150**, 234301 (2019).

[26] R. C. Couto, M. Guarise, A. Nicolaou, N. Jaouen, G. S. Chiuzbaian, J. Lüning, V. Ekholm, J.-E. Rubensson, C. Såthe, F. Hennies, V. Kimberg, F. F. Guimarães, H. Ågren, F. Gel'mukhanov, L. Journel, and M. Simon, Anomalously strong two-electron one-photon X-ray decay transitions in CO caused by vibronic coupling, Sci. Rep. **6**, 20947 (2016).

[27] R. C. Couto, M. Guarise, A. Nicolaou, N. Jaouen, G. S. Chiuzbaian, J. Lüning, V. Ekholm, J.-E. Rubensson, C. Såthe, F. Hennies, V. Kimberg, F. F. Guimarães, H. Ågren, F. Gel'mukhanov, L. Journel, and M. Simon, Coupled electron-nuclear dynamics in resonant $1\sigma \to 2\pi$ X-ray Raman scattering of CO molecule, Phys. Rev. A **93**, 032510 (2016).

[28] R. Schinke, *Photodissociation Dynamics* (Cambridge University Press, Cambridge, U.K., 2009).

[29] D. Céolin, J.-C. Liu, V. Vaz da Cruz, H. Ågren, L. Journele, R. Guillemin, T. Marchenko, R. K. Kushawaha, M. N. Piancastelli, R. Püttner, M. Simon, and F. Gel'mukhanov, Recoil-induced ultrafast molecular rotation probed by dynamical rotational Doppler effect, Proc. Natl. Acad. Sci. USA **116**, 4877 (2019).

[30] J.-C. Liu, V. Vaz da Cruz, S. Polyutov, A. Föhlisch, and F. Gel'mukhanov, Recoil-induced dissociation in hard-X-ray photoionization, Phys. Rev. A **100**, 053408 (2019).

[31] S. Maheshwari, M. B. Fridriksson, S. Seal, J. Meyer, and F. C. Grozema, The Relation between Rotational Dynamics of the Organic Cation and Phase Transitions in Hybrid Halide Perovskites, J. Phys. Chem. C **123**, 14652 (2019).

[32] F. Filsinger, J. Küpper, G. Meijer, J. H. Nielsen, I. Nevo, J. L. Hansen, and H. Stapelfeldt, Quantum-state selection, alignment, and orientation of large molecules using static electric and laser fields, J. Chem. Phys. **131**, 064309 (2009).

[33] K. Lin, I. Tutunnikov, J. Qiang *et al.*, All-optical field-free three-dimensional orientation of asymmetric-top molecules, Nat. Commun. **9**, 5134 (2018).

[34] J. Karczmarek, J. Wright, P. Corkum, and M. Ivanov, Optical Centrifuge for Molecules, Phys. Rev. Lett. **82**, 3420 (1999).

[35] O. M. Sarkisov, D. G. Tovbin, V. V. Lozovoy, F. E. Gostev, A. A. Titov, S. A. Antipin, and S. Y. Umanskiy, Femtosecond Raman-induced polarization spectroscopy of coherent rotational wave packets: D_2, N_2 and NO_2, Chem. Phys. Lett. **303**, 458 (1999).

[36] M. Kubasik, A. Cebo, E. Hertz, R. Chaux, B. Lavorel, and O. Faucher, Shaping of a ground state rotational wavepacket by frequency-chirped pulses, J. Phys. B: At., Mol. Opt. Phys. **34**, 2437 (2001).

[37] V. Kemlin, A. Bonvalet, L. Daniault, and M. Joffre, Transient Two-Dimensional Infrared Spectroscopy in a Vibrational Ladder, J. Phys. Chem. Lett. **7**, 3377 (2016).

[38] L. Monacelli, G. Batignani, G. Fumero, C. Ferrante, S. Mukamel, and T. Scopigno, Manipulating Impulsive Stimulated Raman Spectroscopy with a Chirped Probe Pulse, J. Phys. Chem. Lett. **8**, 966 (2017).

[39] S. B. Zhang and N. Rohringer, Quantum-beat Auger spectroscopy, Phys. Rev. A **92**, 043420 (2015).

[40] E. Allaria, F. Bencivenga, R. Borghes *et al.*, Two-colour pump-probe experiments with a twin- pulse-seed extreme ultraviolet free-electron laser, Nat. Commun. **4**, 2476 (2014).

[41] A. Nilsson, O. Björneholm, E. O. F. Zdansky, H. Tillborg, N. Mårtensson, J. N. Andersen, and R. Nyholm, Photoabsorption and the unoccupied partial density of states of chemisorbed molecules, Chem. Phys. Lett. **197**, 12 (1992).

[42] O. Björneholm, A. Nilsson, E. O. F. Zdansky, A. Sandell, B. Hernnäs, H. Tillborg, J. N. Andersen, and N. Mårtensson, 2π-resonance broadening in X-ray-absorption spectroscopy of adsorbed CO, Phys. Rev. B **46**, 10353 (1992).

[43] A. Föhlisch, J. Hasselström, P. Bennich, N. Wassdahl, O. Karis, A. Nilsson, L. Triguero, M. Nyberg, and L. G. M. Pettersson, Ground-state interpretation of X-ray emission spectroscopy on adsorbates: CO adsorbed on Cu(100), Phys. Rev. B **61**, 16229 (2000).

[44] B. Gilbert, F. Huang, H. Zhang, G. A. Waychunas, and J. F. Banfield, Nanoparticles: Strained and Stiff, Science **305**, 651 (2004).